Supporting Information

Hashimoto et al. 10.1073/pnas.1101488108

SI Results

Presence of Nonfunctional CF Contacts on the PC Soma. We used triple fluorescent labeling of cerebella at P12 and P16 for calbindin (PC marker, blue), VGluT2 (CF terminal marker, green) and anterograde tracer dextran Alexa 594 (DA-594, red) and quantitatively evaluated the pattern and site of CF innervations. We classified PCs into three groups: mono-innervation (*mono*), multiple innervation with surplus CF innervation confined to the soma (*multisoma*), and multiple innervation with surplus CF innervation extending to dendrites (*multidendrite*). However, our initial assessment scored apparently higher ratios of multiple CF innervation in control mice at P12 (98%, 90 of 92 PCs) and P16 (74%, 59 of 80 PCs), compared with the ratios determined by the electrophysiological method (~80% at P10–P12 and ~50% at P16–P18, Fig. 4). We assumed that this apparently higher incidence of multiple CF innervation by morphological examination might be due to the presence of nonfunctional CF contacts on the PC soma which could not be detected by the electrophysiological method. We tested whether perisomatic CF terminals directly contacted PC somata or were separated from somatic membranes with glial sheets by using triple immunofluorescent labeling for calbindin, VGluT2, and plasmalemmal glutamate transporter GLT-1 (astroglial marker) (Fig. S6 *A–D*). In both control and PC-$Ca_v2.1$ KO mice, ~80% of VGluT2-positive perisomatic terminals around the apical half of the PC soma were directly apposed to somatic membranes without intervention of glial sheets at P12 and P16 (Fig. S6 *E* and *F*, black columns). This result indicates that most of the VGluT2-positive perisomatic terminals on the apical half of the PC soma represent functional CF synapses. On the basal half of the PC soma, however, frequency of such direct apposition was consistently low (Fig. S6 *E* and *F*, white columns), particularly in control mice (52.2% at P12 and 20.8% at P16). Thus, more than half of the VGluT2-positive perisomatic terminals on the basal half of the PC soma represent nonfunctional synapses, and including these nonfunctional synapses resulted in overestimation of the incidence of multiple CF innervation. Therefore, in the following morphological evaluation of CF innervation patterns, we included only the VGluT2-positive perisomatic terminals with direct apposition on the apical half of the PC soma.

SI Materials and Methods

Generation of PC-Specific $Ca_v2.1$ Knockout Mice. To generate the $Ca_v2.1$ floxed mice, we isolated a genomic fragment of the $Ca_v2.1$ gene by PCR from C57BL/6 mouse genomic DNA. The 1.8-kb DNA fragment, which carried the 34-bp loxP sequence and neo cassette flanked by two *frt* sites (1), was inserted into the site 274 bp upstream of exon 4. The 34-bp *loxP* sequence with 26-bp linker sequence was inserted into the site 368 bp downstream of exon 4. The targeting vector ptv$Ca_v2.1$-flox contained exon 4 of the $Ca_v2.1$ gene flanked by *loxP* sequences, 7.2 kb upstream and 3.2 kb downstream genomic sequences, and 4.3 kb pMC1DTpA (Fig. 1*A*). Linearized vector was electroporated into RENKA ES cells and recombinant clones were identified by Southern blot hybridization analysis (Fig. 1*B*). Recombinant ES cells were injected into eight-cell stage embryos of the CD-1 mouse strain. Resulting chimeric mice were mated with C57BL/6 mice to establish the $Ca_v2.1$ floxed ($Ca_v2.1^{lox/lox}$) line. Resulting chimeric mice (male) were mated with C57BL/6 mice (female) to generate heterozygous mice ($Ca_v2.1^{lox/+}$). These mice were further mated with each other to create homozygous mice ($Ca_v2.1^{lox/lox}$). To establish the PC-selective $Ca_v2.1$ knockout line, $Ca_v2.1^{lox/lox}$ mice were then mated with D2CreN ($GluD2^{+/Cre}$) mice. For each experiment, male mice ($Ca_v2.1^{lox/lox}$, $GluD2^{+/Cre}$) and female mice ($Ca_v2.1^{lox/lox}$, $GluD2^{+/+}$) were crossed with each other to obtain control ($Ca_v2.1^{lox/lox}$, $GluD2^{+/+}$) and PC-selective $Ca_v2.1$ knockout ($Ca_v2.1^{lox/lox}$, $GluD2^{+/Cre}$, from now on called PC-$Ca_v2.1$ KO) mice.

Recordings from PCs in Cerebellar Slices. Parasagittal cerebellar slices (250 μm) were prepared from mice aged 5–31 d postnatally as described (2). Whole-cell recordings were made from visually identified PC somata using an upright microscope (BX50WI; Olympus) (2, 3). All experiments were carried out at 31 °C except the pharmacological experiment using Ca^{2+} channel blockers that was performed at room temperature. An intracellular solution was composed of (in mM): 60 CsCl, 10 Cs D-gluconate, 20 TEA-Cl, 20 BAPTA, 4 $MgCl_2$, 4 ATP and 30 Hepes (pH 7.3, adjusted with CsOH). The pipette access resistance was compensated by 70–80%. The composition of the standard bathing solution was 125 mM NaCl, 2.5 mM KCl, 2 mM $CaCl_2$, 1 mM $MgSO_4$, 1.25 mM NaH_2PO_4, 26 mM $NaHCO_3$ and 20 mM glucose, bubbled with 95% O_2 and 5% CO_2. For recording CF-EPSCs and Ca^{2+} currents, bicuculline (10 μM) was added to block inhibitory synaptic transmission. For recording IPSCs, 10 μM 2,3-dioxo-6-nitro-1,2,3,4-tetrahydrobenzo quinoxaline-7-sulphonamide (NBQX) and 5 μM (*R*)-3-(2-carboxypiperazin-4-yl)-propyl-1-phosphonic [(*R*)-CPP] were added. The bathing solution used for Ca^{2+} current recording was 50 mM NaCl, 75 mM TEA-Cl, 2.5 mM KCl, 2 mM $CaCl_2$, 1 mM $MgSO_4$, 1.25 mM NaH_2PO_4, 26 mM $NaHCO_3$, 20 mM glucose, and 0.0005 mM tetrodotoxin. For the pharmacological experiment to measure voltage-dependent Ca^{2+} current, $CaCl_2$ and $MgSO_4$ were substituted by equimolar $BaCl_2$ and $MgCl_2$, respectively. Ionic currents were recorded with an Axopatch 1D (Molecular Devices) or an EPC-10 patch clamp amplifier (HEKA Elektronik). The signals were filtered at 2 kHz and digitized at 20 kHz. On-line data acquisition and off-line data analysis were performed using PULSE software (HEKA). Stimulation pipettes were filled with the standard saline. Stimuli (duration, 0.1 ms; amplitude, 0–90 V) were applied at 0.2 Hz. CFs were stimulated in the granule cell layer 50–100 μm away from the Purkinje cell soma. The number of CFs innervating the recorded PC was estimated by the number of discrete CF-EPSC steps (2).

Whole-Cell Recordings and Two-Photon Ca^{2+} Imaging from PCs in Anesthetized Mice. Mice were anesthetized with 1.0–1.5% isoflurane. Targeted whole-cell recordings and somatic and dendritic Ca^{2+} imaging were performed using a two-photon microscope (Ultima IV; Prairie) as previously described (4). The intracellular solution was composed of 130 mM K-gluconate, 10 mM KCl, 10 mM NaCl, 0.5 mM EGTA, 10 mM Hepes, 4 mM Mg-ATP, 0.4 mM Na_2-GTP, 0.05 mM Alexa 594, and 0.1 mM Oregon Green BAPTA-1 (pH 7.3, 285 mOsm). Ca^{2+} imaging was performed >20 min after break-in and the images were acquired at 5–21 frames/s. Ca^{2+} transients were analyzed by ImageJ (http://rsbweb.nih.gov/ij/).

Immunohistochemistry. Under deep pentobarbital anesthesia (100 μg/g of body weight, i.p.), mice were fixed and processed for preparation of parasagittal microslicer sections (50 μm in thickness; VT1000S; Leica). We used goat calbindin antibody (1 μg/mL) and vesicular glutamate transporter 2 (VGluT2) antibody (0.5 μg/mL), whose specificity was reported previously (5, 6). All

immunohistochemical incubations were done at room temperature in a free-floating state. Cerebellar sections were incubated with 10% normal donkey serum for 20 min, a mixture of primary antibodies overnight, and a mixture of Alexa Fluor 488- (Invitrogen) and indocarbocyanine (Cy3) (Jackson Immunoresearch)-labeled species-specific secondary antibodies for 2 h at a dilution of 1:200. Single-plane images were taken with a confocal laser scanning microscope (FV1000; Olympus) and analyzed with Metamorph software (Universal Imaging). The density of CF synaptic terminals on PC somata was evaluated by counting the number of VGluT2-positive puncta on the somatic membrane of PCs. Triple immunofluorescent labeling of cerebellar tissues with calbindin, VGluT2, and GLT-1 (7) antibodies was also used.

In Situ Hybridization. After inhalational anesthesia with diethylether, brains were freshly obtained from control and PC-$Ca_v2.1$ KO mice at P2 and P5 and immediately frozen in powdered dry ice. The day of birth was counted as P0. As probes for the floxed region of $Ca_v2.1$, two antisense oligonucleotides (45-mer) were synthesized and used in mixture. The sequences were 5′-CTCAGTGTCCGTAGGTCAAACTCCGTCCCCACAGTGGCCAAGATG-3′ and 5′-AAACTCCGTCCCGACAGTGGCCAAGATGCCTGTTAGCACCACGAC-3′. They were processed for probe labeling with [^{33}P]dATP using terminal deoxyribonucleotidyl transferase (Invitrogen) to a specific activity of 10,000 dpm/μL. Hybridization was performed as described previously (5). Hybridized sections were exposed either to X-ray films (Kodak BIOMAX MR) for 3 wk or to nuclear track emulsion (NTB2; Kodak) for 4 wk.

Drugs. Bicuculline, NBQX, (*R*)-CPP, and nifedipine were obtained from TOCRIS. ω-Agatoxin IVA and ω-conotoxin GVIA were obtained from Peptide Institute. Tetrodotoxin and cytochrome C were obtained from Nacalai Tesque. Calcium channel blockers were applied with 1mg/mL cytochrome C at room temperature.

Data Analysis. To quantify the disparity in multiple CF-EPSCs recorded in a given PC, we calculated the disparity index from each multiply innervated PC (2). Briefly, the amplitudes of individual CF-EPSCs in a given multiply innervated PC were measured (A_1, A_2,⋯, A_i, ⋯ A_N, $N \geq 2$). N is the number of CFs innervating a given PC. A_i represents the EPSC amplitude for the CF_i at the same holding potential. Parameters were represented by the following formulas:

$$\text{Disparity index} = \frac{\text{SD}}{M}$$

$$M = \frac{1}{N}\sum_{i=1}^{N} A_i$$

$$\text{SD} = \sqrt{\frac{1}{N-1}\sum_{i=1}^{N}(A_i - M)^2}.$$

Statistical Analysis. Averaged data from different experiments are presented as mean ± SEM. Statistical significance was assessed by Mann–Whitney U test. Differences between groups were judged to be significant at $P < 0.05$. $^{*}P < 0.05$ and $^{**}P < 0.01$, respectively.

1. Takeuchi T, et al. (2002) Flp recombinase transgenic mice of C57BL/6 strain for conditional gene targeting. *Biochem Biophys Res Commun* 293:953–957.
2. Hashimoto K, Kano M (2003) Functional differentiation of multiple climbing fiber inputs during synapse elimination in the developing cerebellum. *Neuron* 38:785–796.
3. Edwards FA, Konnerth A, Sakmann B, Takahashi T (1989) A thin slice preparation for patch clamp recordings from neurones of the mammalian central nervous system. *Pflugers Arch* 414:600–612.
4. Kitamura K, Judkewitz B, Kano M, Denk W, Häusser M (2008) Targeted patch-clamp recordings and single-cell electroporation of unlabeled neurons *in vivo*. *Nat Methods* 5:61–67.
5. Miura E, et al. (2006) Expression and distribution of JNK/SAPK-associated scaffold protein JSAP1 in developing and adult mouse brain. *J Neurochem* 97:1431–1446.
6. Miyazaki T, Fukaya M, Shimizu H, Watanabe M (2003) Subtype switching of vesicular glutamate transporters at parallel fibre-Purkinje cell synapses in developing mouse cerebellum. *Eur J Neurosci* 17:2563–2572.
7. Yamada K, et al. (1998) Glutamate transporter GLT-1 is transiently localized on growing axons of the mouse spinal cord before establishing astrocytic expression. *J Neurosci* 18:5706–5713.

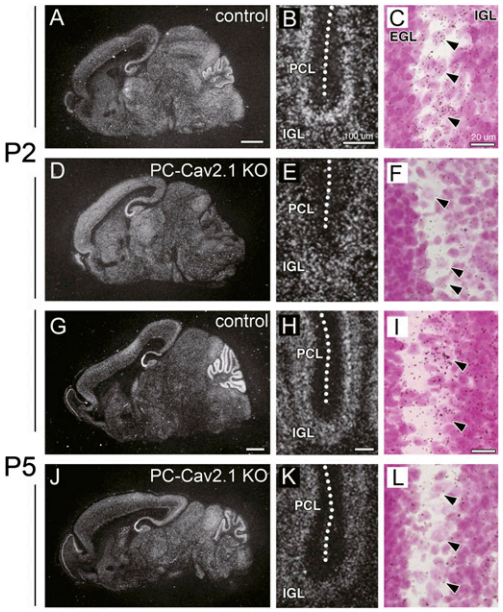

Fig. S1. Distribution of the $Ca_v2.1$ mRNA in control and PC-$Ca_v2.1$ KO mice at P2 and P5. (*A*, *D*, *G*, and *J*) Dark-field micrographs of parasagittal mouse brains. (*B*, *C*, *E*, *F*, *H*, *I*, *K*, and *L*) Dark-field (*B*, *E*, *H*, and *K*) and bright-field (*C*, *F*, *I*, and *L*) micrographs of high-power views of the cerebellar cortex. PCL, Purkinje cell layer; IGL, internal granular layer. Arrowheads indicate PCs. Note that the $Ca_v2.1$ expression in PCL is specifically eliminated in PC-$Ca_v2.1$ KO mice at P2 and P5.

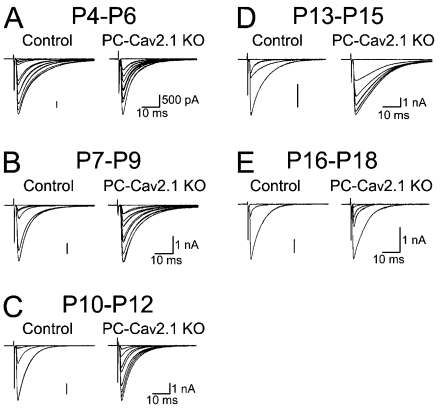

Fig. S2. Representative CF-EPSC traces from PCs of control and PC-$Ca_v2.1$ KO mice at various stages of postnatal cerebellar development. Records were taken from control mice at P6 (*A*, P7 V_h = −30 mV), P7 (*B*, V_h = −30 mV), P11 (*C*, V_h = −20 mV), P15 (*D*, V_h = −20 mV), and P18 (*E*, V_h = −30 mV) and from PC-$Ca_v2.1$ KO mice at P5 (*A*, P7 V_h = −30 mV), P8 (*B*, V_h = −30 mV), P11 (*C*, V_h = −20 mV), P14 (*D*, V_h = −30 mV), and P16 (*E*, V_h = −30 mV).

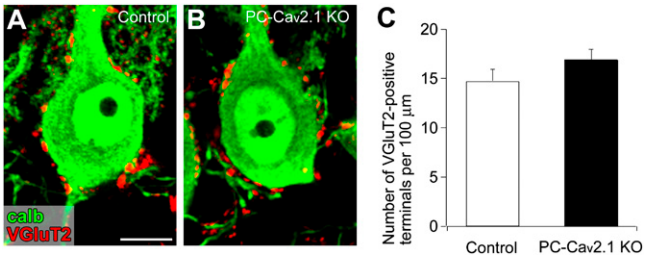

Fig. S3. Density of the CF synaptic terminal on the PC soma. (*A* and *B*) Immunostainings of PCs with a calbindin antibody (green) and CF terminals with a VGluT2 antibody (red) in control (*A*) and PC-$Ca_v2.1$ KO (*B*) PCs. (*C*) Summary bar graph for the number of VGluT2-positive terminals per 100-μm membrane of the PC soma. Numbers of PCs are 149 (four mice) for control and 189 (five mice) for PC-$Ca_v2.1$ KO. Densities of CF terminals were identical between control and PC-$Ca_v2.1$ KO PCs.

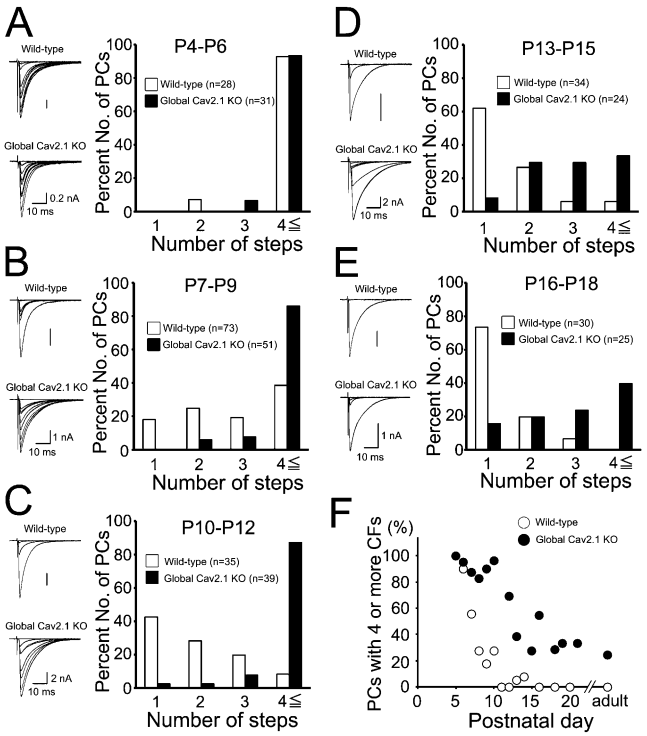

Fig. S4. Impairment of CF synapse elimination during postnatal development in global $Ca_v2.1$ KO mice. (*A*) (*Left*) Specimen records of CF-EPSCs of wild-type [P5; holding potential (V_h) = −40 mV] and global $Ca_v2.1$ KO mice (P5; V_h = −40 mV). One or two traces are superimposed at each threshold intensity. (*Right*) Frequency distribution showing the number of discrete CF-EPSC steps of wild-type (open bars) and global $Ca_v2.1$ KO (solid bars) mice at P4–P6. There is no significant difference between wild-type and global $Ca_v2.1$ KO mice ($P = 0.945$; Mann–Whitney *U* test). (*B–E*) CF innervation at P7–P9 (*B*), P10–P12 (*C*), P13–P15 (*D*), and P16–P18 (*E*) illustrated similarly to *A*. Specimen records were from wild-type mice at P7 (*B*, V_h = −30 mV), P11 (*C*, V_h = −20 mV), P14 (*D*, V_h = −20 mV), and P18 (*E*, V_h = −20 mV) and from global $Ca_v2.1$ KO mice at P8 (*B*, V_h = −20 mV), P10 (*C*, V_h = −30 mV), P15 (*D*, V_h = −20 mV), and P18 (*E*, V_h = −20 mV). Frequency distributions for *B–E* are significantly different between wild-type and global $Ca_v2.1$ KO mice ($P < 0.001$). (*F*) Developmental changes in the fraction of PCs innervated by four or more CFs.

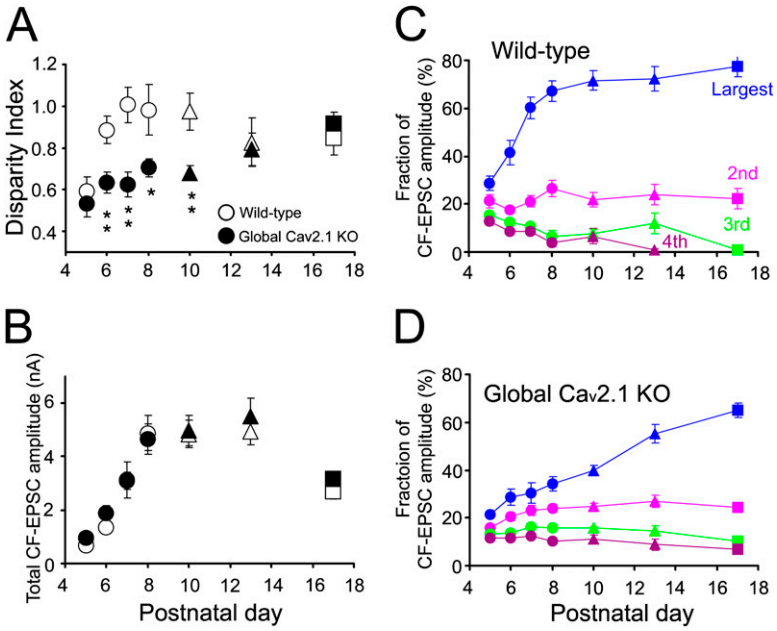

Fig. S5. Impairment of functional differentiation of CF-EPSCs in global $Ca_v2.1$ KO mice. (*A*) Developmental changes in the disparity index. The numbers of PCs for each data point are 9–28 for wild-type (white symbols) and 8–44 for global $Ca_v2.1$ KO (black symbols) mice. Data for P9–P11 and P12–P14 are pooled and indicated with triangles. Data for P15–P21 are pooled and indicated with boxes. (*B*) Developmental changes in the total amplitude of CF-EPSCs (V_h = −20mV) elicited in each PC. Plots include the data for mono-innervating CFs. The numbers of PCs for each data point are 9–41 for wild-type and 8–44 for global $Ca_v2.1$ KO mice. (*C* and *D*) Developmental changes in the fraction of the largest (blue), second (pink), third (green), and fourth (violet) CF-EPSC amplitude relative to the total CF-EPSC amplitude in wild-type (*C*) and global $Ca_v2.1$ KO (*D*) mice.

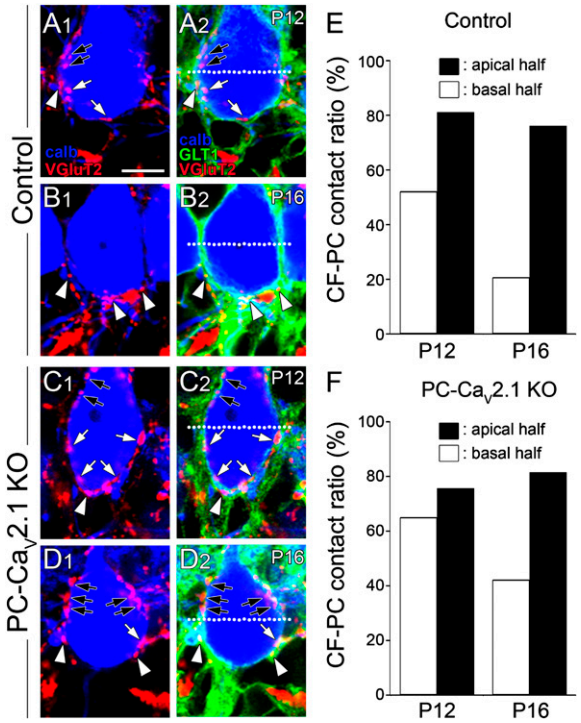

Fig. S6. Perisomatic VGluT2-positive terminals on the apical half, but not the basal half, of PC soma mostly represent direct synaptic contacts (*A*–*D*) Triple immunofluorescence for calbindin (blue), VGluT2 (red), and GLT-1 (green) in control (*A* and *B*) and PC-Ca_v2.1 KO (*C* and *D*) mice at P12 (*A* and *C*) and P16 (*B* and *D*). Dotted lines indicate borders dividing the apical and basal halves of PC somata. Black and white arrows indicate VGluT2-positive terminals on apical and basal halves of PC somata, respectively, which appeared to have direct contacts. White arrowheads indicate VGluT2-positive terminals separated from PC somata with GLT1-positive glial sheets. (*E* and *F*) Histogram showing ratios of direct contact of VGluT2-positive terminals to PC somata in control (*E*) and PC-Ca_v2.1 KO (*F*) mice. Sample sizes for control mice were 819 terminals from 149 PCs (P12) and 906 terminals from 138 PCs (P16). Those for PC-Ca_v2.1 KO mice were 2,189 terminals from 159 PCs (P12) and 1,178 terminals from 125 PCs (P16). (Scale bar, 10 μm.)

Table S1. Kinetics of CF-EPSCs at P18–P31

Genotype	CF group	10–90% rise time, ms	Decay time constant, ms	Amplitude, pA	Chord conductance, nS	Paired-pulse depression, %	*n*
Control	CF-mono	0.4 ± 0.1	7.1 ± 1.3	2193 ± 526	83 ± 30	74.4 ± 14.1	27
	CF-multi-S	0.4 ± 0.1	6.9 ± 1.8	2177 ± 736	95 ± 50	76.4 ± 5.7	22
	CF-multi-W	0.4 ± 0.1	3.6 ± 2.2	404 ± 323	16 ± 13	61.9 ± 11.1	16
PC-Ca_v2.1 KO	CF-multi-S	0.5 ± 0.1**	9.3 ± 3.1**	2444 ± 821	98 ± 36	77.2 ± 7.7	17
	CF-multi-W	0.5 ± 0.1**	4.2 ± 2.5	443 ± 356	16 ± 12	59.4 ± 8.8	16

Data are expressed as mean ± SD. CF-EPSCs are divided into three groups, namely CF-EPSCs from mono-innervated PCs (CF-mono), the largest CF-EPSCs in individual multiply innervated PCs (CF-multi-S), and other smaller CF-EPSCs in individual multiply innervated PCs (CF-multi-W). $^{**}P < 0.01$ (comparison between the values of the corresponding CF groups, Mann–Whitney *U* test). Amplitudes are measured at V_h = −20 mV. Chord conductance is calculated from the amplitudes recorded at V_h = −20 mV and +40 mV. Ratio of paired-pulse depression is calculated from the first and second EPSC amplitudes elicited by two successive stimuli at an interval of 50 ms.

Table S2. Spontaneous IPSCs in PCs at P6–P7

	Control	PC-Ca_v2.1 KO
P6–P7		
Frequency, Hz	3.9 ± 3.0	3.4 ± 3.7
Amplitude, pA	64.7 ± 31.3	79.4 ± 37.6
No.	9	9
P10		
Frequency, Hz	30.0 ± 14.2	39.5 ± 14.5
Amplitude, pA	541.4 ± 298.9	425.0 ± 352.2
No.	6	6

Data are expressed as mean ± SD. No significant difference is reported between control and PC-Ca_v2.1 KO mice pairs (Mann–Whitney *U* test).